

Ligand-Field Spin-Orbit Energy Levels in the d^5 Electron Configuration of Octahedral and Tetrahedral Symmetry

E. König *, R. Schnakig, and S. Kremer

Institute of Physical Chemistry II, University of Erlangen-Nürnberg,
D-8520 Erlangen, Germany

(Z. Naturforsch. **29 a**, 419–428 [1974]; received 16 November 1973)

The complete ligand-field, Coulomb interelectronic repulsion, and spin-orbit interaction matrices have been derived for the d^5 electron configuration within octahedral (O_h) and tetrahedral (T_d) symmetry. The calculations were performed in both the weak-field and strong-field coupling schemes and complete agreement of the results was achieved. The energy matrices are parametrically dependent on ligand field (Dq), Coulomb repulsion (B , C), and spin-orbit interaction (ζ). Correct energy diagrams are presented which display the splittings by spin-orbit perturbation as well as the effect of configuration mixing. Applications to the interpretation of electronic spectra, and to complete studies in magnetism are pointed out. The detailed behavior at the crossover of ground terms is considered.

1. Introduction

Recently, two of the present authors¹ reported the results of calculations on the combined ligand field and spin-orbit interactions for the d^4 , d^6 electronic configurations in octahedral and tetrahedral symmetry. Similar calculations ("complete ligand field theory") for the more simple d^2 , d^8 and d^3 , d^7 electronic configurations have been known^{2,3} for some time and have shown their usefulness in the interpretation of electronic absorption and emission spectra as well as in general considerations of the electronic structure of suitable transition metal compounds. As far as the d^5 configuration is concerned, matrix elements in both the strong-field⁴ and the weak-field⁵ coupling scheme have been reported. However, since nothing is known about detailed numerical calculations, the correctness of these purely algebraic results has not been established beyond doubt. In fact, as will be shown below, one of the previous studies contains numerous errors in the reported matrix elements of both the spin-orbit and the ligand field interactions. The few attempts that have been advanced in the past at the interpretation of electronic spectra⁶ in general employed energy levels without spin-orbit coupling and with partial neglect of configuration interaction. Notable exceptions exist. Thus Low and Rosengarten⁷ diagonalized the complete d^5 problem for a number of parameter sets specifically chosen to fit the electronic spectra of MnF_2 , $MnCl_2$, and of the Fe^{3+} ion in hydrates. In an attempt to interpret the spectra of

hydrated manganous chlorides, Goode⁸ carried out a limited spin-orbit interaction calculation on the basis of the matrix elements of Schroeder⁴. These matrices were likewise employed by Vala et al.⁹ in order to explain the spectra of the tetrahedral complexes $[(CH_3)_4N]_2MnCl_4$ and $[(CH_3)_4N]_2MnBr_4$. Neither of these studies is of general utility. Also, it should be noted that, in the d^6 configuration at least, interaction with high lying energy levels seriously affects even the nature of the electronic ground state in certain cases¹⁰. It follows that the correct inclusion of configuration interaction may be a factor of importance in any assignment of spectral transition energies. On the other hand, spin-orbit interaction produces, if considered separately, only minor splittings and energy shifts within the 3d transition metal series, while it is known to be a major energy contribution in systems containing 4d or 5d transition metal ions.

In the present study, we have rederived the complete energy levels of the d^5 electron configuration in ligand fields of octahedral and tetrahedral symmetry. Complete spin-orbit and configuration interaction has been included and the derivation has been performed in both the weak-field and the strong-field coupling schemes. Subsequently, the correctness of the results has been established by extended cross-checks of detailed numerical data computed within the two equivalent formalisms. Finally, employment of the available matrix elements^{4,5} demonstrates their correctness or otherwise. Detailed applications of the results to the interpretation of electronic spectra and other experimental data will be reported separately.

* Reprint requests to Doz. Dr. E. König, Institut für Physikal. Chemie II der Universität Erlangen-Nürnberg, D-8520 Erlangen, Egerlandstraße 3.



2. Theoretical Basis

The Hamiltonian appropriate to the present study includes the operators of Coulomb interelectronic repulsion, spin-orbit interaction, and octahedral (or tetrahedral) ligand field potential

$$\mathcal{H} = \sum_i \left\{ -\frac{\hbar^2}{2m} \nabla_i^2 - \frac{Ze^2}{r_i} + \xi(r_i) \mathbf{s}_i \cdot \mathbf{l}_i \right\} + \sum_{i>j} \frac{e^2}{r_{ij}} + V_{\text{LF}}(r, \theta, \varphi). \quad (1)$$

The summations in Eq. (1) extend over the five d electrons, all quantities having their usual meaning. The ligand field potential $V_{\text{LF}}(r, \theta, \varphi)$ of octahedral symmetry, if acting on a single electron, assumes the explicit form

$$V_{\text{oct}}^i = \frac{7}{2} \{ C_0^{(4)}(\theta, \varphi) + (\frac{5}{14})^{1/2} \cdot [C_4^{(4)}(\theta, \varphi) + C_{-4}^{(4)}(\theta, \varphi)] \} \frac{Ze^2}{R^5} r^4. \quad (2)$$

Here, $C_q^{(k)}$ are the rationalized spherical harmonics¹¹ defined by their relation to the more common spherical harmonics Y_{kq} ,

$$C_q^{(k)} = \left(\frac{4\pi}{2k+1} \right)^{1/2} Y_{kq}. \quad (3)$$

In the calculations to follow, two different coupling schemes will be employed. These differ by the order according to which the last three terms of Eq. (1) are considered as a perturbation. Thus, in weak-field coupling, the sequence is

$$\sum_{i>j} e^2/r_{ij} > \sum_i \xi(r_i) \mathbf{s}_i \cdot \mathbf{l}_i > V_{\text{LF}}(r, \theta, \varphi) \quad (4)$$

whereas in strong-field coupling we use the sequence

$$V_{\text{LF}}(r, \theta, \varphi) > \sum_{i>j} e^2/r_{ij} > \sum_i \xi(r_i) \mathbf{s}_i \cdot \mathbf{l}_i. \quad (5)$$

If all state functions of the d⁵ configuration are properly included, both formalisms produce identical eigenvalues of the energy. After all, the results obtained in the two coupling schemes differ alone by the characterization of the final energy levels.

3. Weak-field Coupling

Wave Functions: In the five-electron problem, the usual procedure¹² of setting-up symmetry adapted cubic wave functions in coordinate space is extremely cumbersome if not difficult. Similar to the d⁴, d⁶ configuration¹, vector coupling techniques have thus been preferred. Wave functions conforming to the

total Hamiltonian of Eq. (1) and transforming according to irreducible representation Γ , component γ (of the molecular point group) are then given by

$$|v S L J \Gamma \gamma a\rangle = \sum_{M_J} |v S L J M_J\rangle \langle J M_J | J \Gamma \gamma a\rangle. \quad (6)$$

Here, v is the seniority number, the expansion coefficients $\langle J M_J | J \Gamma \gamma a\rangle$ may be determined, e. g., by the projection operator technique¹³, and the label a (branching multiplicity index) is used to distinguish functions of the same Γ , i. e. if Γ occurs more than once in the reduction $D^{(J)}(\mathbf{G}) \rightarrow \sum_i a_i^{(J)} \Gamma_i$. For details of determination of the functions $|v S L J M_J\rangle$ refer to a previous paper¹.

Matrix Elements: Since the Coulomb interelectronic repulsion operator commutes with the symmetry operators of the molecular point group as well as with the angular momentum operators corresponding to \mathbf{L}^2 , \mathbf{S}^2 , and \mathbf{J}^2 , the matrix elements will be independent of J , Γ , γ , and a ,

$$\begin{aligned} \langle v S L J \Gamma \gamma a | \sum_{i>j} \frac{e^2}{r_{ij}} | v' S' L' J' \Gamma' \gamma' a' \rangle &= \\ = \langle v S L | \sum_{i>j} \frac{e^2}{r_{ij}} | v' S' L' \rangle \delta(J, J') \delta(\Gamma, \Gamma') \cdot \\ \cdot \delta(\gamma, \gamma') \delta(a, a'). \end{aligned} \quad (7)$$

The Coulomb operator being determined by the sum of two-electron operators $\mathbf{G} = \sum_{i>j} e^2/r_{ij}$, the matrix elements $\langle u | \mathbf{G} | v \rangle$ vanish, whenever u and v differ in the coordinates of more than two electrons. In the usual approach, the three cases are then distinguished where u and v are either identical or where these differ by one or by two single-electron functions¹⁴. In case of equivalent electrons, the individual non-vanishing matrix elements may be expressed as

$$\begin{aligned} \langle (n l)^2 S L | \frac{e^2}{r_{12}} | (n l)^2 S L \rangle &= \\ = \sum_k (-1)^L \langle l || \mathbf{C}^{(k)} || l \rangle^2 \left\{ \begin{matrix} l & l & k \\ l & l & l \end{matrix} \right\} F^k(n l, n l). \end{aligned} \quad (8)$$

Here, the reduced matrix elements of the irreducible tensor operators $\mathbf{C}^{(k)}$ are simply

$$\langle l || \mathbf{C}^{(k)} || l' \rangle = (-1)^l [(2l+1)(2l'+1)]^{1/2} \begin{pmatrix} l & k & l' \\ 0 & 0 & 0 \end{pmatrix} \quad (9)$$

the quantity in braces is the usual 6- j symbol¹⁵, and the radial integrals $F^k(n l, n l)$ may be conveniently

redefined¹⁴ in terms of the Racah parameters

$$A = F^0 - \frac{1}{9} F^4, \quad B = \frac{1}{49} F^2 - \frac{5}{441} F^4, \quad C = \frac{5}{63} F^4. \quad (10)$$

In Eq. (8), we have taken into account that the matrix elements will be diagonal in L and S , although off-diagonal elements may arise since they will not be diagonal in v .

The matrix elements of spin-orbit interaction may be written

$$\begin{aligned} \langle v S L J I \gamma a | \sum_i \xi(r_i) \mathbf{s}_i \cdot \mathbf{l}_i | v' S' L' J' I' \gamma' a' \rangle \\ = (-1)^{J+L+S'} [l(l+1)(2l+1)]^{1/2} \begin{Bmatrix} L & L' & 1 \\ S' & S & J \end{Bmatrix} \\ \cdot \langle v S L \| \mathbf{V}^{(11)} \| v' S' L' \rangle \cdot \delta(J, J') \delta(I, I') \\ \cdot \delta(\gamma, \gamma') \delta(a, a') \zeta_{nl}. \end{aligned} \quad (11)$$

Here, ζ_{nl} is the spin-orbit coupling parameter and the reduced matrix element of the double tensor operator $\mathbf{V}^{(11)}$ may be expressed as

$$\begin{aligned} \langle v S L \| \mathbf{V}^{(11)} \| v' S' L' \rangle \\ = (-1)^{S+L+s+l} N [s(s+1)[S][L][S']][L']^{1/2} \\ \cdot \sum_{\bar{v} \bar{S} \bar{L}} (-1)^{\bar{S}+\bar{L}} \begin{Bmatrix} S & S' & 1 \\ s & s & \bar{S} \end{Bmatrix} \begin{Bmatrix} L & L' & 1 \\ l & l & \bar{L} \end{Bmatrix} \\ \langle v S L \{ |\bar{v} \bar{S} \bar{L}\rangle \langle \bar{v} \bar{S} \bar{L}| \} v' S' L' \rangle. \end{aligned} \quad (12)$$

In Eq. (12), N is the number of d electrons, $[j]$ denotes the dimension of j , i.e. $2j+1$, the quantities $\langle \bar{v} \bar{S} \bar{L} | \{ v S L \rangle$ are coefficients of fractional parentage¹⁶, and the barred states $\bar{v} \bar{S} \bar{L}$ of l^{N-1} are the parents of state $v S L$ of l^N .

The single-electron ligand field potential V_{LF}^i may be expressed in terms of the tensor operators $\mathbf{C}_q^{(k)}$. The resulting general expression for matrix elements of V_{LF} has been given elsewhere¹. In octahedral symmetry, the expansion of V_{oct}^i in terms of the $\mathbf{C}_q^{(k)}$ is determined by Equation (2). The matrix elements of the octahedral ligand field potential then result as

$$\begin{aligned} \langle v S L J I \gamma a | V_{oct} | v' S' L' J' I' \gamma' a' \rangle \\ = (-1)^{S+L'} 3(70)^{1/2} [(2J+1)(2J'+1)]^{1/2} \begin{Bmatrix} J & J' & 4 \\ L' & L & S \end{Bmatrix} \\ \times \langle v S L \| \mathbf{U}^{(4)} \| v' S' L' \rangle \sum_{MM'} (-1)^M \langle J I \gamma a | J M \rangle \\ \times \left\{ \begin{pmatrix} J & 4 & J' \\ -M & 0 & M' \end{pmatrix} + \left(\frac{5}{14} \right)^{1/2} \left[\begin{pmatrix} J & 4 & J' \\ -M & 4 & M' \end{pmatrix} \right. \right. \\ \left. \left. + \begin{pmatrix} J & 4 & J' \\ -M & -4 & M' \end{pmatrix} \right] \right\} \times \langle J' M' | J' I' \gamma' a' \rangle \\ \cdot \delta(I, I') \delta(\gamma, \gamma') \delta(S, S') D_q. \end{aligned} \quad (13)$$

Here, the expansion coefficients $\langle J M | J I \gamma a \rangle$ are defined by Eq. (6), $\langle v S L \| \mathbf{U}^{(4)} \| v' S' L' \rangle$ is a

reduced matrix element of the unit tensor operator $\mathbf{U}^{(4)}$ and D_q the octahedral splitting parameter. The reduced matrix element of $\mathbf{U}^{(4)}$ may be written as

$$\begin{aligned} \langle v S L | \mathbf{U}^{(4)} | v' S' L' \rangle \\ = (-1)^{L+L'} N [(2L+1)(2L'+1)]^{1/2} \\ \cdot \sum_{\bar{v} \bar{S} \bar{L}} (-1)^{\bar{L}} \langle v S L \{ |\bar{v} \bar{S} \bar{L}\rangle \langle \bar{v} \bar{S} \bar{L}| \} v' S' L' \rangle \\ \cdot \begin{Bmatrix} L & l & \bar{L} \\ l & L' & 4 \end{Bmatrix} \end{aligned} \quad (14)$$

where the significance of the various quantities has been discussed above.

The perturbation matrices for the combined Coulomb, spin-orbit, and ligand field interactions within the d^5 configuration subject to a field of O_h symmetry may then be constructed by combination of Eq. (7), Eq. (11), and Equation (13). The reduced matrix elements may be calculated on the basis of Eq. (9), Eq. (12), and Eq. (14) or alternately they may be obtained directly from one of the tables available in literature¹⁶⁻¹⁸. If published tables are being used, it should be observed that there is an error in the relevant matrix elements of $\mathbf{V}^{(11)}$ in reference¹⁶. * Unfortunately, this error has been reproduced in a recent reference volume¹⁹. In addition, in Slater's tabulation (viz. Table A21-4 of¹⁸), the off-diagonal element of $\sum_{i>j} e^2/r_{ij}$ should be taken as **

$$\left\langle d^5, {}^2D \left\| \sum_{i>j} \frac{e^2}{r_{ij}} \right\| d^5, {}^2D \right\rangle = -6(14)^{1/2} B \quad (15)$$

in order to be consistent with the phases of Racah used here.

Due to the half-integral value of the total spin S , the basis functions $|J I \gamma a\rangle$ [viz. Eq. (6)] where $1/2 \leq J \leq 13/2$ have to be characterized by irreducible representations of the double group dO . The resulting blocked matrices which are of dimension 20, 22, and 42, then belong to Γ_6 , Γ_7 , and Γ_8 of dO , respectively.

4. Strong-field Coupling

Wave Functions. The one-electron functions $t_{2g}(\xi, \eta, \zeta)$ and $e_g(\epsilon, \theta)$ transforming according to the two irreducible representations of the octahedral group are well known. Five different (strong-field) configurations may then be set up, and these are, in

* In Table XIV of¹⁶, it should read correctly

$$\langle d^5, {}^4F \| (30)^{1/2} V^{(11)} \| d^5, {}^4G \rangle = -2(15)^{1/2}.$$

** Cf. also Reference¹⁷.

order of increasing energy: $(t_{2g})^5$; $(t_{2g})^4(e_g)$; $(t_{2g})^3(e_g)^2$; $(t_{2g})^2(e_g)^3$; and $(t_{2g})(e_g)^4$. Functions corresponding to the combined effect of the ligand field and Coulomb interactions [viz. the first two terms of Eq. (5)] are obtained by step-wise coupling of one-electron functions, taking two at a time, finally giving

$$\begin{aligned} & |t_{2g}^m(S_1 \Gamma_1) e_g^n(S_2 \Gamma_2), S M_S \Gamma \gamma\rangle \\ &= \sum_{M_{S1} M_{S2} \gamma_1 \gamma_2} |t_{2g}^m S_1 M_{S1} \Gamma_1 \gamma_1\rangle |e_g^n S_2 M_{S2} \Gamma_2 \gamma_2\rangle \\ & \cdot \langle \Gamma_1 \gamma_1 \Gamma_2 \gamma_2 | \Gamma \gamma \rangle \langle S_1 M_{S1} S_2 M_{S2} | S M_S \rangle. \end{aligned} \quad (16)$$

The terms arising from the octahedral d^5 system are listed below:

$$\begin{aligned} (t_{2g})^5: & \quad {}^2T_2 \\ (t_{2g})^4(e_g): & \quad {}^4T_1, {}^4T_2, {}^2A_1, {}^2A_2, \\ & \quad 2 {}^2E, 2 {}^2T_1, 2 {}^2T_2 \\ (t_{2g})^3(e_g)^2: & \quad {}^6A_1, 2 {}^4E, {}^4T_1, {}^4T_2, \\ & \quad {}^4A_1, {}^4A_2, 2 {}^2A_1, \\ & \quad {}^2A_2, 3 {}^2E, 4 {}^2T_1, 4 {}^2T_2 \\ (t_{2g})^2(e_g)^3: & \quad {}^4T_1, {}^4T_2, {}^2A_1, {}^2A_2, \\ & \quad 2 {}^2E, 2 {}^2T_1, 2 {}^2T_2 \\ (t_{2g})(e_g)^4: & \quad {}^2T_2 \end{aligned}$$

All these terms are g according to parity. Finally, "total" state functions corresponding to the combined effect of the ligand field, Coulomb repulsion, and spin-orbit interactions may be expressed by

$$\begin{aligned} |\alpha S \Gamma \Gamma_T \gamma_T b\rangle &= \sum_{M_S \gamma} |\alpha S M_S \Gamma \gamma\rangle \\ & \cdot \langle S M_S \Gamma \gamma | \Gamma_T \gamma_T b \rangle. \end{aligned} \quad (17)$$

These functions transform according to Γ_T where Γ_T results from the subduction of the direct product of spin and space representations, viz. $\Gamma_S \otimes \Gamma = \sum b_T \Gamma_T$. In Eq. (17), α represents any additional quantum numbers which may be required and b is a Kronecker multiplicity index with respect to Γ_T .

Matrix Elements. The ligand field interaction within the one-electron cubic basis $\{t_{2g}, e_g\}$ is diagonal, the corresponding matrix elements being simply

$$\begin{aligned} \langle t_{2g} | V_{\text{oct}} | t_{2g} \rangle &= -4 Dq, \\ \langle e_g | V_{\text{oct}} | e_g \rangle &= 6 Dq \end{aligned} \quad (18)$$

where $Dq = (1/6)(Z e^2/R^5) \langle r^4 \rangle$. The ligand field energy of a particular strong-field configuration is the algebraic sum of the matrix elements of Equation (18).

The Coulomb interelectronic repulsion energy may be calculated similar to weak-field coupling²⁰, the non-zero matrix elements being finally expressed in

terms of the parameters A , B , and C [cf. Equation (10)].

Matrix elements of spin-orbit interaction may be expressed, by application of the generalized Wigner-Eckart theorem to the functions of Eq. (17), according to

$$\begin{aligned} \langle \alpha S \Gamma \Gamma_T \gamma_T b | \sum_i \xi(r_i) \mathbf{s}_i \cdot \mathbf{l}_i | \alpha' S' \Gamma' \Gamma_T' \gamma_T' b' \rangle \\ = c(S \Gamma S' \Gamma', b b' \Gamma_T) \\ \cdot \langle \alpha S \Gamma | \sum_i \xi(r_i) \mathbf{s}_i \cdot \mathbf{l}_i | \alpha' S' \Gamma' \rangle \\ \times \delta(\Gamma_T, \Gamma_T') \delta(\gamma_T, \gamma_T'). \end{aligned} \quad (19)$$

The coefficients $c(S \Gamma S' \Gamma', b b' \Gamma_T)$ which are comparable to Racah coefficients in $SO(3)$ have been introduced by Griffith²¹. These quantities may be determined on the basis of the following system of homogeneous equations

$$\begin{aligned} \langle \alpha S M_S \Gamma \gamma | \sum_i \xi(r_i) \mathbf{s}_i \cdot \mathbf{l}_i | \alpha' S' M_S' \Gamma' \gamma' \rangle \\ = \langle \alpha S \Gamma | \sum_i \xi(r_i) \mathbf{s}_i \cdot \mathbf{l}_i | \alpha' S' \Gamma' \rangle \delta(M_S, M_S') \\ \cdot \delta(\gamma, \gamma') \times \sum_{\substack{\Gamma_T \gamma_T \\ b b'}} c(S \Gamma S' \Gamma', b b' \Gamma_T) \\ \cdot \langle S M_S \Gamma \gamma | \Gamma_T \gamma_T b \rangle \langle \Gamma_T \gamma_T b' | S' M_S' \Gamma' \gamma' \rangle. \end{aligned} \quad (20)$$

The perturbation matrices for the combined octahedral ligand field, Coulomb, and spin-orbit interactions within the d^5 configuration may then be constructed by using the appropriate multiples of Eq. (18) in combination with Eq. (8) and Equation (19). The blocked matrices thus obtained are characterized by the irreducible representations Γ_6 , Γ_7 , and Γ_8 and are of the same dimensions as in weak-field coupling.

5. Intercomparison of Weak-field and Strong-field Calculations and Previous Treatments

The complete perturbation matrices resulting from the weak-field and the strong-field formalism differ alone by a similarity transformation

$$\mathcal{H}(S, t_{2g}^m e_g^n, \Gamma_i) = \mathbf{U}(\Gamma_i)^{-1} \mathcal{H}(S, L, J, \Gamma_i) \mathbf{U}(\Gamma_i). \quad (21)$$

In Eq. (21), the transformation matrix $\mathbf{U}(\Gamma_i)$ connects the corresponding energy matrices for irreducible representation Γ_i . It follows that, if complete configuration interaction is included, weak-field and strong-field coupling approaches are only parametrically distinct. Therefore, identical results should be obtained from both treatments upon numerical substitution. This fact provides a powerful

means to check the correctness of the derived results. Additional checks are available if one of the three interactions is set equal to zero. The results expected for these limiting cases are well known.

The resulting Γ_6 , Γ_7 , and Γ_8 matrices of the octahedral d^5 problem were intercompared for various sets of values of the parameters B , C , ζ , and Dq and complete agreement between the weak-field and strong-field treatments was found. The same conclusion follows from a study of the limiting cases. In addition, it was demonstrated, by an independent calculation, that the matrices of Schroeder⁴ produce eigenvalues which are identical to those obtained in the present study. The previously published d^5 strong-field matrices are therefore correct.

On the other hand, if the published weak-field matrix elements of Li^5 are employed in a parallel calculation, significant discrepancies are encountered. A careful recalculation of the algebra of the weak-field coupling approach located a number of errors in the published⁵ matrices.* These include systematic errors which are caused by the failure to recognize the effect of the Kronecker symbol $\delta(a, a')$

* In order to facilitate comparison between the two sets of weak-field results, the phases of the wave functions were such chosen as to agree, as closely as possible, with those of Li^5 . Difficulties still occur with repeated representations. Thus there are two states Γ_8 with $J=11/2$ and two of each Γ_7 and Γ_8 with $J=13/2$. In this case, the original functions of Li were employed which are linear combinations of the corresponding functions in the present study.

** In Γ_7 , the spin-orbit interaction matrix element given below should read correctly as

$$\left\langle {}^4\text{F}_{2\frac{1}{2}} \left| \sum_i \xi(r_i) \mathbf{S}_i \cdot \mathbf{L}_i \right| {}^2\text{F}_{2\frac{1}{2}} \right\rangle = - (5(2)^{1/2}/6) \zeta_{\text{nd}}.$$

The correct values of the erroneous matrix elements of ligand field interaction are as follows.

In Γ_6 :

$$\langle {}^2\text{I}_{5\frac{1}{2}} | V_{\text{oct}} | {}^2\text{H}_{4\frac{1}{2}} \rangle = - (32(455)^{1/2}/143) Dq$$

In Γ_7 :

$$\langle {}^2\text{I}_{6\frac{1}{2}} | V_{\text{oct}} | {}^2\text{F}_{3\frac{1}{2}} \rangle = (15(66)^{1/2}/77) Dq$$

$$\langle {}^2\text{I}_{6\frac{1}{2}} | V_{\text{oct}} | {}^2\text{D}_{2\frac{1}{2}} \rangle = (60(22)^{1/2}/77) Dq$$

$$\langle {}^2\text{I}_{6\frac{1}{2}} | V_{\text{oct}} | {}^2\text{H}_{5\frac{1}{2}} \rangle = - (48(385)^{1/2}/77) Dq$$

$$\langle {}^2\text{I}_{6\frac{1}{2}} | V_{\text{oct}} | {}^2\text{G}_{3\frac{1}{2}} \rangle = - ((110)^{1/2}/77) Dq$$

$$\langle {}^2\text{I}_{6\frac{1}{2}} | V_{\text{oct}} | {}^2\text{F}_{2\frac{1}{2}} \rangle = (30(22)^{1/2}/77) Dq$$

In Γ_8 :

$$\langle {}^4\text{F}_{4\frac{1}{2}} | V_{\text{oct}} | {}^4\text{D}_{2\frac{1}{2}} \rangle = - (9(35)^{1/2}/49) Dq$$

$$\langle {}^2\text{F}_{2\frac{1}{2}} | V_{\text{oct}} | {}^2\text{D}_{2\frac{1}{2}} \rangle = - (20(7)^{1/2}/21) Dq$$

$$\langle {}^2\text{G}_{3\frac{1}{2}} | V_{\text{oct}} | {}^2\text{G}_{4\frac{1}{2}} \rangle = (20(110)^{1/2}/77) Dq$$

$$\langle {}^2\text{G}_{4\frac{1}{2}} | V_{\text{oct}} | {}^2\text{D}_{1\frac{1}{2}} \rangle = (3(55)^{1/2}/11) Dq$$

of Equation (11). These corrections have been listed in an erratum by Li²². In addition, there are errors in the numerical values of matrix elements of both spin-orbit and ligand field interactions.**

6. Energy Level Diagrams

In Fig. 1 an energy level diagram is presented for the d^5 electron configuration subject to a ligand field of octahedral symmetry. The parameter values employed are $B = 825 \text{ cm}^{-1}$, $C = 4 B$, and $\zeta = 400 \text{ cm}^{-1}$. These values for B , C , and ζ are approximately suitable for hexahydrated complex ions of the $3d^5$ configuration***. Since the diagram is plotted as function of Dq , predictions for complex ions with ligands different from H_2O are still possible, provided the parameters B , C , and ζ are not much different from those assumed here†. As is well known, the ligand field splitting parameters in tetrahedral and octahedral fields are related by

$$Dq_{\text{tet}} = - \frac{4}{9} Dq_{\text{oct}}. \quad (22)$$

Therefore, the matrices employed in octahedral symmetry may be used in the case of tetrahedral sym-

In addition, all matrix elements of ligand field interaction in Tables 1, 2, and 3 of⁵ as well as those listed above have to be multiplied by the phase factor $(-1)^{L-L'+J-J'}$ in order to obtain the correct eigenvalues from the combined matrices.

*** A least squares fit of the emission spectrum²³ of the Mn^{2+} ion produces $B = 960 \text{ cm}^{-1}$, $C = 3325 \text{ cm}^{-1}$, whereas only the estimate $B \sim 1090 \text{ cm}^{-1}$ is known for Fe^{3+} . The nephelauxetic ratio in $\text{M}(\text{H}_2\text{O})_6^{n+}$ is $\beta \sim 0.88$ if $n = 2$ and $\beta \sim 0.75$ if $n = 3$. The chosen value of B is the average of the resulting B_{complex} . The splitting of the free ion ^6S ground term gives $\zeta = 347 \text{ cm}^{-1}$ in Mn^{2+} , and $\zeta \sim 460 \text{ cm}^{-1}$ has been extrapolated for Fe^{3+} . Again the chosen value of ζ is the approximate average of these two values.

† The designation of terms in Fig. 1 and Fig. 2 does not imply pure configurational states. Indeed, some mixing by CI and by spin-orbit interaction is often present. Since this mixing is dependent on Dq , the notation corresponds to the largest contribution at $Dq = 3000 \text{ cm}^{-1}$. For illustration purposes, we give below the (highest) percentage content of that eigenfunction which corresponds to the term designation given in Figure 1.

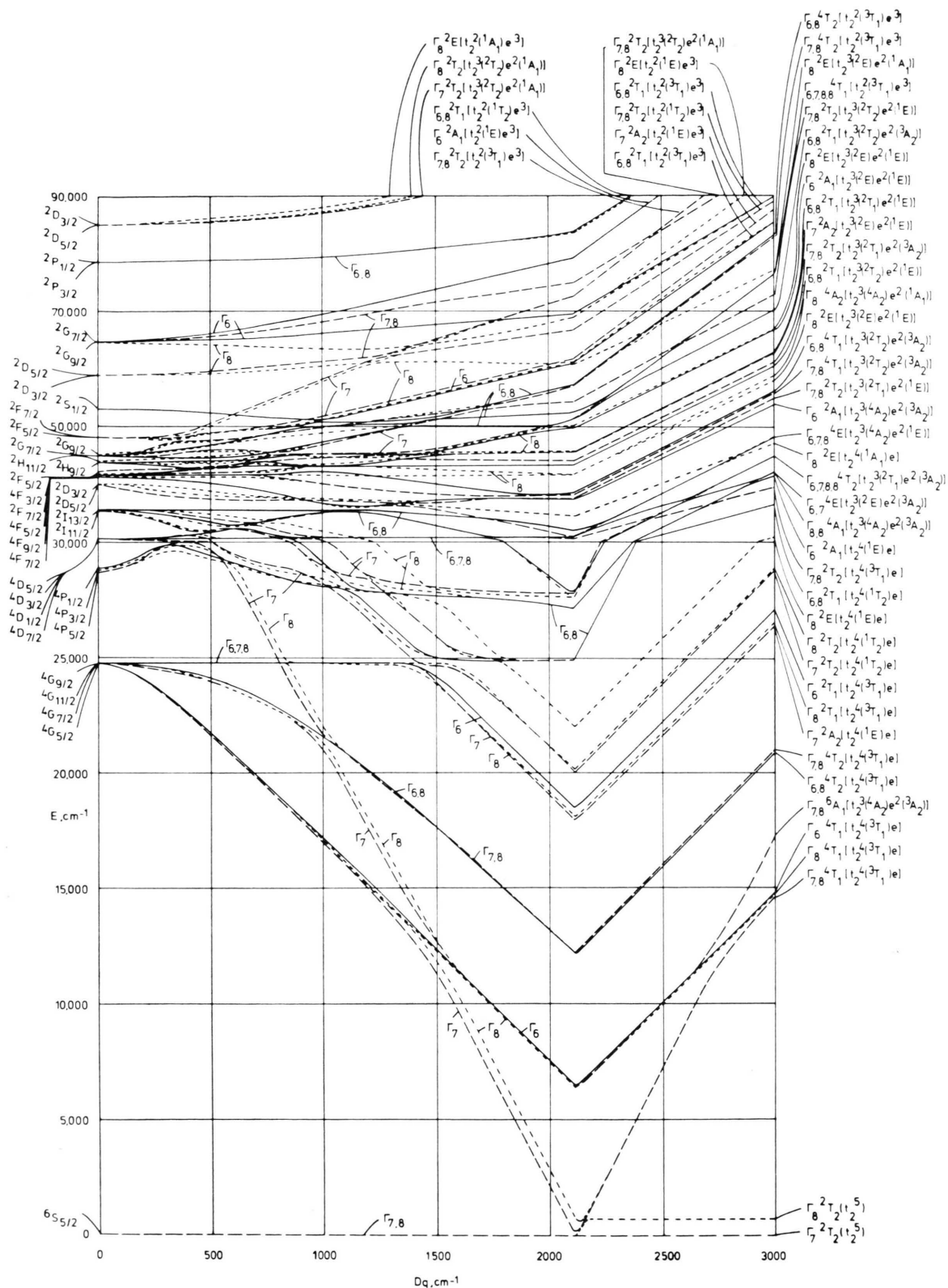
$$35 \pm 2.5\%: \Gamma_8[{}^2\text{E}(t_2^3({}^2\text{E})e^2({}^1\text{E}))];$$

$$40 \pm 2.5\%: \begin{aligned} &\Gamma_6, \Gamma_8[{}^2\text{T}_1(t_2^2({}^3\text{T}_1)e^3)] \\ &\Gamma_7, \Gamma_8, \Gamma_8[{}^2\text{T}_2(t_2^2({}^1\text{T}_2)e^3)] \\ &\Gamma_7[{}^2\text{T}_2(t_2^3({}^2\text{T}_2)e^2({}^1\text{A}_1))] \\ &\Gamma_8[{}^4\text{A}_1(t_2^3({}^4\text{A}_2)e^2({}^3\text{A}_2))]; \end{aligned}$$

$$50 \pm 2.5\%: \begin{aligned} &\Gamma_6, \Gamma_8[{}^2\text{T}_1(t_2^3({}^2\text{T}_2)e^2({}^1\text{E}))] \\ &\Gamma_8[{}^2\text{T}_1(t_2^2({}^3\text{T}_1)e^3)] \end{aligned}$$

$$55 \pm 2.5\%: \begin{aligned} &\Gamma_6, \Gamma_7[{}^4\text{E}(t_2^3({}^2\text{E})e^2({}^3\text{A}_2))] \\ &\Gamma_6, \Gamma_7, \Gamma_8[{}^4\text{E}(t_2^3({}^4\text{A}_2)e^2({}^1\text{E}))] \\ &\Gamma_6[{}^2\text{T}_1(t_2^2({}^3\text{T}_1)e^3)] \\ &\Gamma_8[{}^2\text{E}(t_2^4({}^1\text{A}_1)e)] \\ &\Gamma_8[{}^2\text{E}(t_2^3({}^2\text{E})e^2({}^1\text{E}))]. \end{aligned}$$

No listing implies 60% or higher content.



d^5 -octahedral: $B = 825 \text{ cm}^{-1}$, $C = 4B$, $\zeta = 400 \text{ cm}^{-1}$

Fig. 1. Energy level diagram for the d^5 configuration in an octahedral field including spin-orbit coupling: $B = 825 \text{ cm}^{-1}$, $C = 4B$, $\zeta = 400 \text{ cm}^{-1}$. The designation of the terms by the strong-field configurational labels and their parent terms corresponds to the largest contribution which is present at the Dq value assumed at the right end of the diagram. The labels have to be supplemented with g subscripts for O_h symmetry.

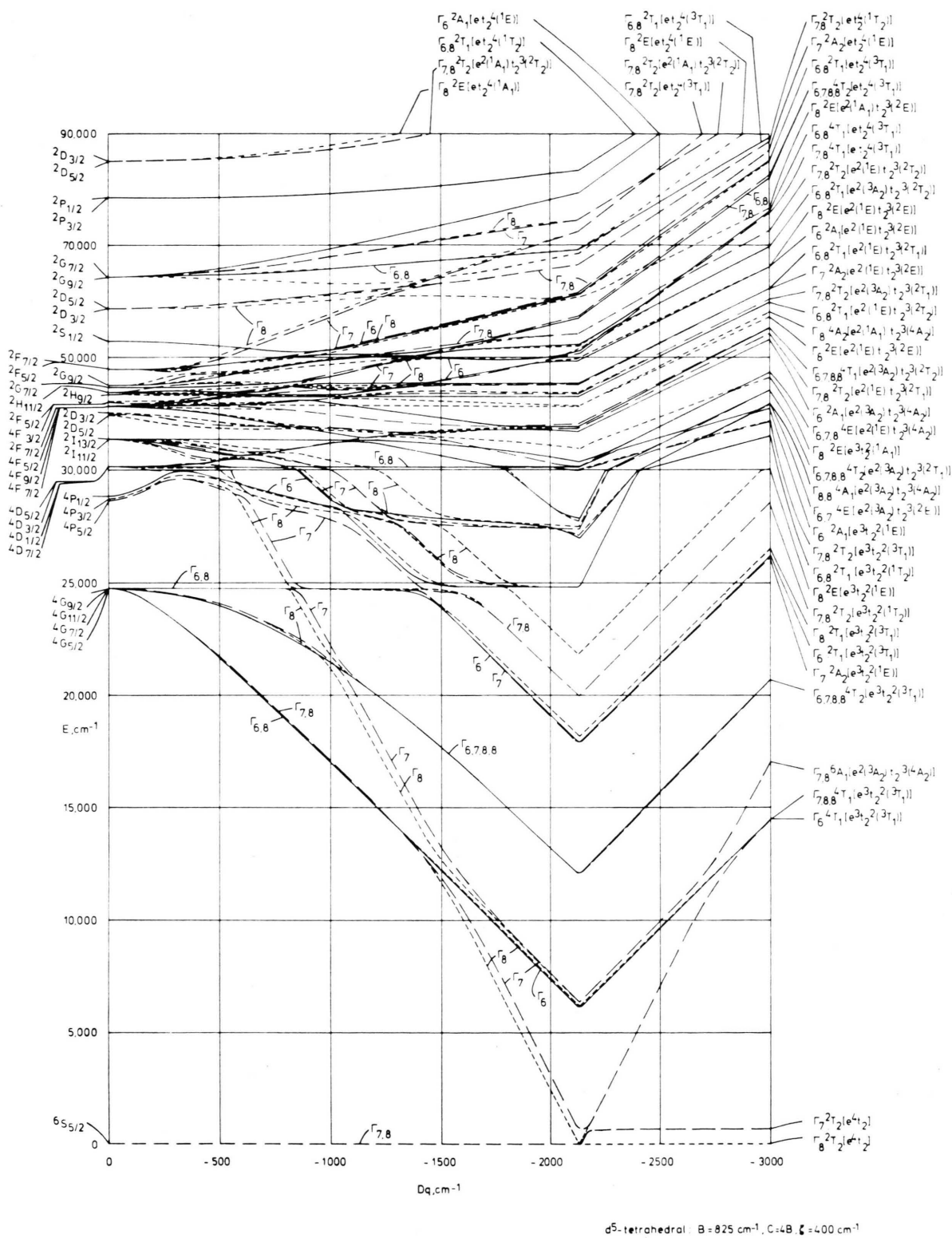


Fig. 2. Energy level diagram for the d^5 configuration in a tetrahedral field including spin-orbit coupling: $B = 825 \text{ cm}^{-1}$, $C = 4B$, $\zeta = 400 \text{ cm}^{-1}$. Refer to caption of Fig. 1 for further details.

metry as well if a sign change of Dq is effected. The results which are obtained for the same set of the parameters B , C , and ζ are displayed in the diagram of Figure 2. It is evident that the octahedral and tetrahedral complete ligand field diagrams are different. This is due to the fact that, although the electron-hole conjugation implies

$$\begin{aligned} E(d^n, Dq, B, C) &= E(d^{10-n}, -Dq, B, C), \\ E(d^n, -Dq, B, C) &= E(d^{10-n}, Dq, B, C) \end{aligned} \quad (23)$$

it is certainly

$$E(d^5, Dq, \zeta, B, C) \neq E(d^5, -Dq, \zeta, B, C).$$

The diagrams presented here demonstrate the effect of spin-orbit interaction on the various energy terms of the d^5 configuration. * The changes consist of (i) term splittings which are first-order effects (diagonal matrix elements only) and (ii) term shifts which are of second or higher order (off-diagonal matrix elements). The energy levels displayed here will be useful in the interpretation of the electronic spectra of suitable complex compounds and solids, particularly at cryogenic temperatures. For a specific application, the parameters, B , C , ζ , and Dq would be assigned values which produce a best fit to the experimental data. If the effect of the interactions is to be discussed in a general way, it has proved sufficient to have available energy level diagrams¹⁻³ for just one fixed set of values of B , C , and ζ and for varying Dq as in Fig. 1 and Figure 2.

In addition, the present results may be used as the starting point in a complete calculation of paramagnetic susceptibilities. This calculation presents magnetic data as function of the semi-empirical spectroscopic parameters employed here, i. e. B , C , ζ , and Dq ²⁴. A similar study on the d^4 , d^6 configuration has been reported previously²⁵.

7. Crossover Behavior

In the two situations studied here, viz. the octahedral and tetrahedral d^5 configuration, two ground states of different spin are formed. In octahedral symmetry, the change of ground state from ${}^6A_1(t_2^3 e^2)$ to ${}^2T_2(t_2^5)$ takes place if

$$10 Dq > 7\frac{1}{2} B + 5 C + CI \quad (24)$$

* The corresponding results in the limit of zero spin-orbit interaction have been given by Y. Tanabe and S. Sugano, J. Phys. Soc. Japan **9**, 766 [1954] and the resulting diagrams are reproduced in numerous books and review articles.

where CI is the energy of configuration interaction affecting the ${}^2T_2(t_2^5)$ term only²⁶. In tetrahedral symmetry, the expressions of the conjugate hole configuration have to be employed. These crossover energies are influenced, in addition, by spin-orbit interaction as has been demonstrated in case of the d^4 , d^6 configuration²⁷. The detailed behavior of the levels at the crossover in d^5 systems is likewise of interest, since relevant experimental data are known²⁸. Figure 3 therefore shows the central region of the complete octahedral d^5 diagram and in Fig. 4 the corresponding plot for a tetrahedral d^5 ion is presented. The detailed data of Fig. 3 may be compared with results of a limited calculation by de Lisle and Golding²⁹ in Fig. 3 of that paper.

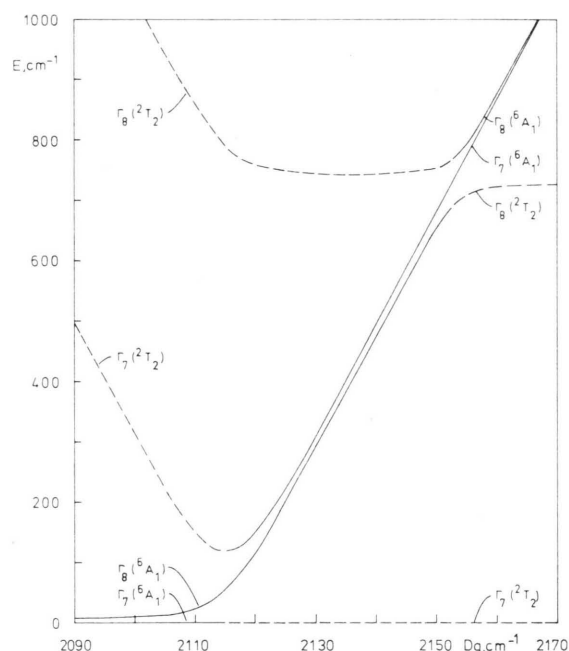


Fig. 3. Lowest energy levels for the octahedral d^5 system in the region of the crossover (i. e. at $10 Dq = 21,150 \text{ cm}^{-1}$). Parameters used are as in Figure 1.

If spin-orbit coupling is included, the terms involved in the crossover are thus split according to ${}^6A_1 \rightarrow \Gamma_7 + \Gamma_8$ and ${}^2T_2 \rightarrow \Gamma_7 + \Gamma_8$. Also, it should be realized that the ${}^2T_2(t_2^5)$ term interacts with nine higher energy 2T_2 terms, while the ${}^6A_1(t_2^3 e^2)$ is pure. Thus, in the neighborhood of the crossover, both the Γ_7 and Γ_8 levels will be considerably mixed by spin-orbit interaction. With $10 Dq$ approaching the crossover more closely, the amount of inter-

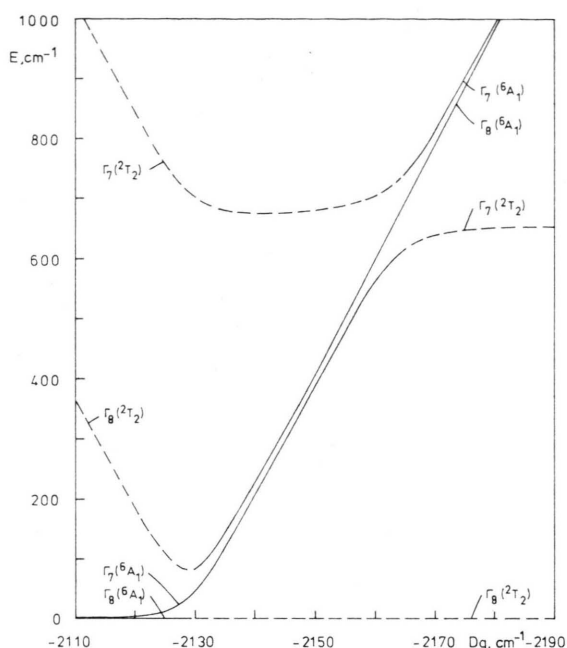


Fig. 4. Lowest energy levels for the tetrahedral d⁵ system in the region of the crossover (i. e. at $10 Dq = -21,300 \text{ cm}^{-1}$). Parameters used are as in Figure 2.

mixing rises progressively. Thus, if $10 Dq = 20,900 \text{ cm}^{-1}$ (left side of Fig. 3) is assumed, the lowest level Γ_7 at 0.0 cm^{-1} consists of 97.71% ${}^6A_1[t_2^3(4A_2)e^2(3A_2)]$, 1.26% ${}^2T_2(t_2^5)$, and 1.03% various other contributions, whereas the Γ_7 level at 496.0 cm^{-1} is composed of 92.22% ${}^2T_2(t_2^5)$, 3.14% ${}^2T_2[t_2^4(3T_1)e]$, and 4.64% other contributions, cf. Figure 3. The Γ_8 levels at 5.64 cm^{-1} and 1221.4 cm^{-1} are 99.13% and 93.97% pure ${}^6A_1[t_2^3(4A_2)e^2(3A_2)]$ and pure ${}^2T_2(t_2^5)$, respectively. Let us consider the situation again at $10 Dq = 21,150 \text{ cm}^{-1}$. Here, the lowest Γ_7 level still at 0.0 cm^{-1} consists of 50.74% ${}^6A_1[t_2^3(4A_2)e^2(3A_2)]$

and 44.88% ${}^2T_2(t_2^5)$, whereas the second Γ_7 level, now at 119.0 cm^{-1} , is 48.75% ${}^2T_2(t_2^5)$ and 48.47% ${}^6A_1[t_2^3(4A_2)e^2(3A_2)]$. Obviously, at $10 Dq = 21,175 \text{ cm}^{-1}$, the next $10 Dq$ studied, the $\Gamma_7[{}^2T_2(t_2^5)]$ has become ground state with 62.65% pure ${}^2T_2(t_2^5)$ and 31.98% ${}^6A_1[t_2^3(4A_2)e^2(3A_2)]$. If we decide to define the crossover by that value of $10 Dq$ where, in the lowest Γ_7 level, equal contributions from the ${}^6A_1[t_2^3(4A_2)e^2(3A_2)]$ and ${}^2T_2(t_2^5)$ terms are involved, the crossover is, within good approximation, at $21,150 \text{ cm}^{-1}$. However, at this value of $10 Dq$, the two Γ_8 levels are still 98.89% and 93.95% pure ${}^6A_1[t_2^3(4A_2)e^2(3A_2)]$ and pure ${}^2T_2(t_2^5)$, respectively. The condition of equal contributions is here satisfied alone between $10 Dq = 21,525 \text{ cm}^{-1}$, and $10 Dq = 21,550 \text{ cm}^{-1}$, cf. Figure 3. Thus if $10 Dq = 21,525 \text{ cm}^{-1}$ the Γ_8 level at 686.3 cm^{-1} consists of 59.26% ${}^6A_1[t_2^3(4A_2)e^2(3A_2)]$ and 37.34% ${}^2T_2(t_2^5)$, whereas the other Γ_8 level at 765.2 cm^{-1} is composed of 57.02% ${}^2T_2(t_2^5)$ and 39.83% ${}^6A_1[t_2^3(4A_2)e^2(3A_2)]$. Approximately reversed contributions are obtained at $10 Dq = 21,550 \text{ cm}^{-1}$. There is apparently a region of about 375 cm^{-1} within that the levels Γ_7 and Γ_8 cross. In this respect, the situation is similar to, e. g., the octahedral d⁴ configuration²⁷.

As can be seen from Fig. 4, the behavior of the tetrahedral d⁵ configuration at the crossover is quite similar to that in the octahedral case and is therefore not discussed here in detail. Observe that the lowest level is here a Γ_8 and that the crossover appears, in good approximation, at $10 Dq = -21,300 \text{ cm}^{-1}$.

Acknowledgements

The authors appreciate financial support by the Deutsche Forschungsgemeinschaft, the Stiftung Volkswagenwerk, and the Fonds der Chemischen Industrie.

- ¹ E. König and S. Kremer, Z. Naturforsch., in the press.
- ² A. D. Liehr and C. J. Ballhausen, Ann. Phys. **6**, 134 [1959].
- ³ A. D. Liehr, J. Phys. Chem. **67**, 1314 [1963].
- ⁴ K. A. Schroeder, J. Chem. Phys. **37**, 1587 [1962].
- ⁵ Wai-Kee Li, Spectrochim. Acta **24 A**, 1573 [1968].
- ⁶ For a review viz. N. S. Hush and R. J. M. Hobbs, Progr. Inorg. Chem. **10**, 259 [1968].
- ⁷ W. Low and G. Rosengarten, J. Mol. Spectrosc. **12**, 319 [1964].
- ⁸ D. H. Goode, J. Chem. Phys. **43**, 2830 [1965].
- ⁹ M. T. Vala, C. I. Ballhausen, R. Dingle, and S. L. Holt, Mol. Phys. **23**, 217 [1972].
- ¹⁰ E. König and R. Schnakig, Theor. Chim. Acta **30**, 205 [1973].
- ¹¹ G. Racah, Phys. Rev. **62**, 438 [1942].

- ¹² See, for instance, C. J. Ballhausen, Introduction to Ligand Field Theory, McGraw-Hill, New York 1962.
- ¹³ E. König and S. Kremer, Theor. Chim. Acta **32**, 27 [1973].
- ¹⁴ E. U. Condon and G. H. Shortley, The Theory of Atomic Spectra, Cambridge University Press 1935.
- ¹⁵ M. Rotenberg, R. Bivins, N. Metropolis, and J. K. Wooten, The 3-j and 6-j Symbols, The MIT Press, Cambridge, Mass. 1960.
- ¹⁶ G. Racah, Phys. Rev. **63**, 367 [1943].
- ¹⁷ C. W. Nielson and G. F. Koster, Spectroscopic Coefficients for the pⁿ, dⁿ, and fⁿ Configurations, MIT Press, Cambridge, Mass. 1963.
- ¹⁸ J. C. Slater, Quantum Theory of Atomic Structure, Vol. II, McGraw-Hill, New York 1960.
- ¹⁹ I. I. Sobelman, An Introduction to the Theory of Atomic Spectra, Pergamon Press, London 1972.

- ²⁰ Y. Tanabe and S. Sugano, J. Phys. Soc. Japan **9**, 753 [1954].
- ²¹ J. S. Griffith, The Theory of Transition Metal Ions, Cambridge University Press 1961.
- ²² Wai-Kee Li, Spectrochim. Acta **27 A**, 2289 [1971].
- ²³ C. E. Moore, Atomic Energy Levels, US National Bureau of Standards Circular No. 467, Washington, D. C. 1949, 1952, 1958.
- ²⁴ E. König and S. Kremer, Ber. Bunsenges. Phys. Chem., in the press.
- ²⁵ E. König and S. Kremer, Ber. Bunsenges. Phys. Chem. **76**, 870 [1972].
- ²⁶ E. König and S. Kremer, Theor. Chim. Acta **23**, 12 [1971].
- ²⁷ E. König and S. Kremer, Theor. Chim. Acta **26**, 311 [1972].
- ²⁸ E. König, Ber. Bunsenges. Phys. Chem. **76**, 975 [1972].
- ²⁹ J. M. de Lisle and R. M. Golding, Proc. Roy. Soc. London **A 296**, 457 [1967].